Gupta, Mahendra Kumar; Subbarao, P. M. V.

Article

Development of a semi-analytical model to select a suitable airfoil section for blades of horizontal axis hydrokinetic turbine

Energy Reports

Provided in Cooperation with:
Elsevier

Suggested Citation: Gupta, Mahendra Kumar; Subbarao, P. M. V. (2020) : Development of a semi-analytical model to select a suitable airfoil section for blades of horizontal axis hydrokinetic turbine, Energy Reports, ISSN 2352-4847, Elsevier, Amsterdam, Vol. 6, Iss. 1, pp. 32-37, https://doi.org/10.1016/j.egyr.2019.08.014

Available online at www.sciencedirect.com
ScienceDirect
Energy Reports 6 (2020) 32–37
www.elsevier.com/locate/egyr

6th International Conference on Energy and Environment Research, ICEER 2019, 22–25 July, University of Aveiro, Portugal

Development of a semi-analytical model to select a suitable airfoil section for blades of horizontal axis hydrokinetic turbine

Mahendra Kumar Gupta*, P.M.V. Subbarao

Department of Mechanical Engineering, Indian Institute of Technology Delhi, New Delhi, 110016, India

Received 29 July 2019; accepted 16 August 2019

Abstract

All modern hydro-kinetic turbines are being designed based on a lift, using airfoils, which should have a significant lift to drag ratio to achieve maximum efficiency.SG604X family airfoil has significant lift-to-drag ratio under an operating range of *Re* from 10^5–10^6, which also come under our working conditions. Blade Element Momentum (BEM) theory was used to obtain optimum blade shape. The iterative numerical approach was used in MATLAB to calculate optimized blade profile and coefficient of performance (C_p). After grid independency test, finally k-ω shear stress transport (SST) and the k-ϵ model with enhanced wall treatment were used for calculation of the lift coefficient and the drag coefficient of airfoil SG6043. The performance of the rotor overall expected tip speed ratio (T.S.R (λ)) was calculated and found that maximum $C_{p,max}$ is 0.51 at optimum λ_{opt} of 5. The suitability of SG6043 airfoil over NACA0012 airfoil in our case has been shown.

Peer-review under responsibility of the scientific committee of the 6th International Conference on Energy and Environment Research, ICEER 2019.

Keywords: Blade element momentum theory; Coefficient of performance; Computational fluid dynamics; Horizontal-axis hydrokinetic turbine

1. Introduction

Conventional hydropower plant requires a high head of water to drive turbines, but what if, there are zero head or little head of water. A feasible solution to this lies in hydrokinetic turbines (HKT). HKT systems are electromechanical energy converters that convert the kinetic energy of river streams, tidal currents and human-made water channels into other usable forms of energy.

1.1. Hydro-kinetic turbine's principle

The energy conversion principle of HKT and wind turbines is the same. So for the study of free flow hydrokinetic turbines, the corresponding parameters of wind turbines can be used [1]. The amount of hydro-kinetic power

* Corresponding author.
E-mail address: mahendra.kr.gupta@gmail.com (M.K. Gupta).

https://doi.org/10.1016/j.egyr.2019.08.014

Peer-review under responsibility of the scientific committee of the 6th International Conference on Energy and Environment Research, ICEER 2019.

available for extraction depends on the fluid velocity (V_o), rotor swept area (A) and density of the fluid (ρ). The power coefficient (C_p) determines the performance of HKT as expressed in Eq. (1) [2]. The typical overall efficiency for a hydrokinetic turbine with low mechanical losses is approximately 30% [3]. The performance of HKT depends primarily on these design parameters, tip speed ratio (TSR), solidity (σ) and blade pitch angle (θ_p). The T.S.R (λ) expressed in Eq. (2) is defined as the ratio of the blade tip speed to the free stream fluid velocity (V_o). The Solidity is related to the radius (R), blade chord length (c), and some blades (B), and it is the ratio of the planform area of the blades to the swept area as expressed in Eq. (3).

Generally, a low solidity axial flow turbine turns at a higher TSR than a high solidity turbine, results in higher rotational speed for the same diameter and current speed. However, solidity should be kept around 30% to produce enough starting torque, as demonstrated by the Brazilian and Australian experiences [2,3].

$$C_p = \frac{P}{(1/2)\rho A V_o^3} = \frac{Rotor\ Power}{Power\ in\ the\ water\ current} \tag{1}$$

$$\lambda = \frac{\Omega R}{V_o} \tag{2}$$

$$\sigma = \frac{Bc}{2\pi R} \tag{3}$$

Hydrokinetic energy converters can be divided into lift based and drag based machines. The maximum power coefficient, which can be achieved in a drag based device, is 0.29, which is significantly lower than the Betz limit of 0.593 [4]. Hence, all modern hydrokinetic turbines are being designed on lift principles, using airfoils which should have a significant lift to drag ratio to achieve maximum C_p. Comprehensive reviews on HKT including detailed fundamental studies and turbine classification can be found in [5,6].

Among HKT, small capacity turbines generally come in the range of 1–10 kW. These small turbines compare to the giant turbines differ significantly in terms of operating Reynolds numbers (R_e). The R_e for the turbine under 5 kW is between 10^5–10^6. From the literature, it can be stated that for the small capacity HKT, many have opted that airfoil which was designed either for a large wind turbine or other applications [7–9].

There is no reasonable procedure to choose the appropriate airfoil for HAHkT rotor, because of the wide range of angle of attack (α) over which a blade operates. An effort was made in designing the airfoil to enhance the performance of small wind energy systems. Four airfoils (SG6040, SG6041, SG6042 and SG6043) were wind-tunnel tested at R_e between 10^5 to 10^6. The results showed that small variable-speed wind turbines should benefit from the use of these new airfoils, which provide improved lift-to-drag ratio performance as compared with previously existing airfoils [10]. Hence these airfoils are suitable and being used in our work because it was designed for the same operating conditions.

2. Blade design and modeling

When modeling the performance of HAHkT designs, the most employed method is the Blade Element Momentum theory (BEM) [11–13]. In this theory, the rotor blade is divided into some elemental sections, and the torque is calculated from equating the blade forces generated by these blade elements to the momentum changes occurring in the fluid through the rotor disk. Fig. 1 shows the velocity diagram for the current configuration, where V_{rel} is the relative velocity; the combination of axial fluid velocity (U_a), and tangential fluid velocity due to the rotation (U_t). The angle between chord and rotor plane, between the rotor plane and V_{rel} and between chord and V_{rel} are local pitch angle (θ), flow angle ($\emptyset$) and angle of attack (α), respectively. The blade geometry for an

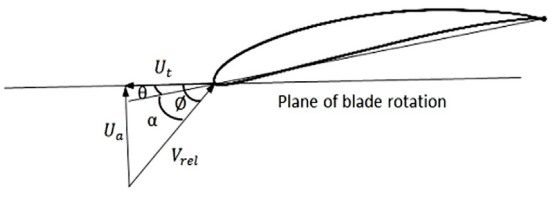

Fig. 1. Velocity diagram for airfoil.

optimum rotor was calculated using the BEM theory with the incorporation of Prandtl's tip loss correction factor to account for losses due to fluid flow from the pressure side to suction side at the blade's tip [14].

Table 1. Blade designed data.

Design parameters	Values
Rated power (W)	1000
Nominal water current velocity (m/s)	2
Design TSR (λ)	4
Number of blades	3
Airfoils	SG6043

The fixed point iterative numerical approach was used in MATLAB to calculate optimized blade profile, and C_p. Blade designed data are shown in Table 1. The performance of the rotor overall expected tip speed ratio (T.S.R (λ)) was calculated and found that maximum $C_{p,max}$ is 0.51 at optimum λ_{opt} of 5. Blade geometry was calculated for this optimum TSR and of blade pitch angle 3.3 degree, which is shown in Table 2.

Table 2. Local pitch angle and chord distribution along blade.

r [m]	α [°]	θ [°]	[°]	c [m]
0.2	3.5	16.2	19.7	0.096
0.24	3.5	13.8	17.3	0.086
0.28	3.5	11.7	15.2	0.078
0.32	3.5	9.8	13.3	0.070
0.36	3.5	8.2	11.6	0.063
0.4	3.5	6.8	10.2	0.056
0.44	3.4	5.6	9.0	0.051
0.48	3.3	4.7	8.0	0.046
0.52	3.1	4.0	7.1	0.041
0.56	2.6	3.5	6.1	0.038
0.6	2.5	3.3	5.8	0.035

3. Computational domain specification and meshing for CFD analysis

The two-dimensional calculations of the SG6043 airfoil were performed using ANSYS-Fluent computational fluid dynamics (CFD) software. To improve the stability of the numerical simulations, the outer boundary in C-Mesh as shown in Fig. 2 was extended 20 chord lengths after the airfoil. ICEM meshing tool was used to generate the unstructured grids in the domain. To capture the boundary layer effect, the high-resolution structured grids were generated around the airfoils. Convergence criteria for x, y, and z momentum, k and ω were set to 1e−06.

As a starting point for 3D simulation of the rotor, CFD analysis was done first with NACA 0012 airfoil and then with SG6043 airfoil on the tapered blade without a twist, having chord length at the root (.096 m) and tip (.035 m) of the blade. As shown in Fig. 3, the computational domain consists of two cylinders; the inner cylinder is extending 7.5 rotor diameters and the outer one ten rotor diameters, respectively, in the axial direction. The rotor is placed inside the inner cylinder. The hub is not included in this model.

A tetrahedral/hybrid mesh was created in the entire domain using ICEM meshing tool. The inner cylinder is rotating while the outer one is stationary. Velocity inlet and pressure outlet boundary conditions (b.c.) were set. The

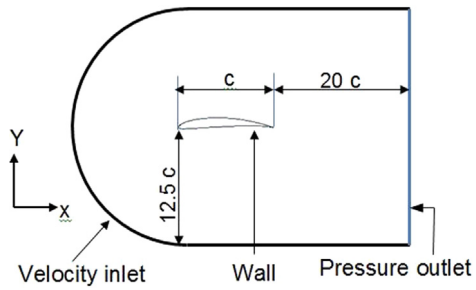

Fig. 2. 2D computational domain with boundary condition.

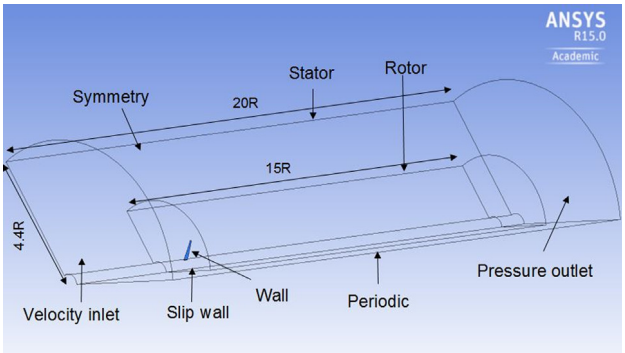

Fig. 3. 3D computational domain with boundary conditions.

symmetry b.c. was applied on top of the stator. The pressure outlet b.c. with atmospheric pressure was applied on the right surface of the outer one. Using periodicity, the flow was simulated around one blade and extrapolated the solution to two more blades to visualize the results for a three-bladed rotor. A moving reference frame (MRF) was incorporated to take into account the rotational effect of the rotor because the unsteady flow field becomes steady w.r.t. MRF. The assumed water current flows towards the positive x-direction at 2 m/s, which is mean flow velocity. This incoming flow is assumed to rotate the blade about the x-axis (the blade is thus spinning counter-clockwise when looking at it from the front).

At standard conditions (20 ^{o}C) the density and viscosity of water are 998.29 kg/m^3 and 1.003×10^{-3} (Pa s) respectively. Amongst different turbulence model, SST k-ω model was used. Second order UPWIND scheme was used for discretization, and the SIMPLE algorithm was selected for solving pressure-velocity coupling. The PRESTO scheme was adopted due to its superiority for flows with steep pressure gradients as the present case [15].

4. Results of numerical analysis

Among various turbulent models available in the ANSYS-Fluent, three different turbulent models were investigated for six different near wall grid spacing around the airfoils — see Fig. 4. The results were compared to the XFoil software packages and wind-tunnel test [10]. After grid independency test, k-ω shear stress transport (SST) and the k-ϵ model with enhanced wall treatment were used for calculation of C_l and C_d and found that the k-ω SST model is in good agreement both for C_l and C_d — see Fig. 5.

Airfoil characteristics of both SG6043 and NACA 0012 airfoils have been shown in Table 3. In Table 4, the calculated torque for the rotor with two different airfoils NACA0012 and SG6043 has been compared. When the rotor was stationary, the torque was zero, and 9.67 N m for NACA0012 airfoil and SG6043 airfoil, respectively,

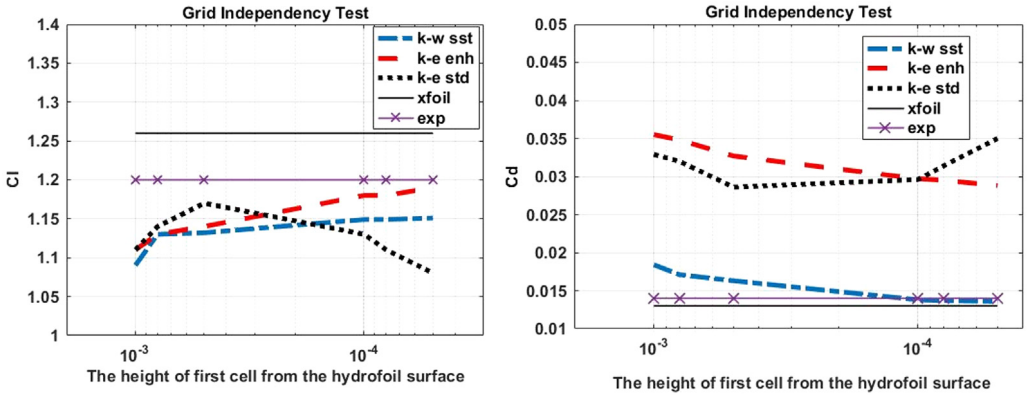

Fig. 4. Lift and drag coefficient at α=5^{o} and R_e=2×10^5.

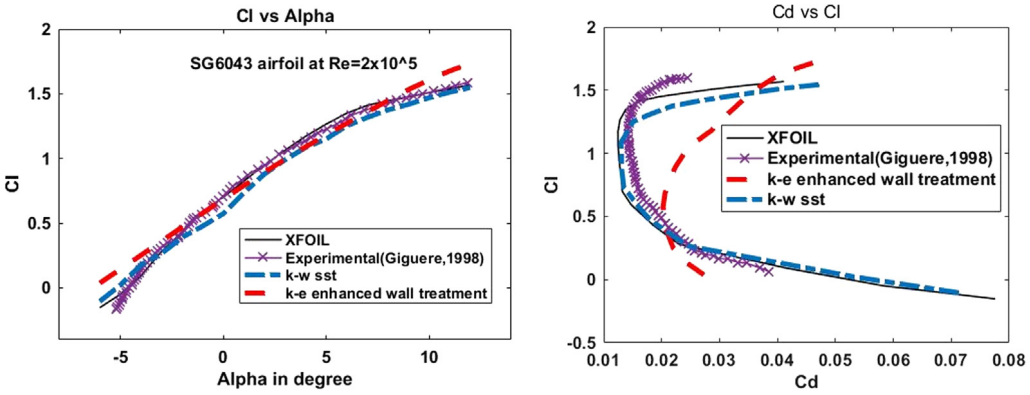

Fig. 5. Comparison of lift and drag coefficient between experimental and fluent at R_e=2×10^5.

Table 3. Airfoil characteristics at $R_e = 2 \times 10^5$, Airfoiltools.com.

Parameters	Thickness	Camber	Max (C_l/C_d)	Stall angle
SG6043	10%	5.5%	98.01	5.5
NACA0012	12.0%	0.0%	47.43	5

Table 4. Comparison of torque for two different airfoil.

Ω (rad/s)	Torque (N m) for one blade of the turbine	
	Blade with NACA0012	Blade with SG6043
0	0.03	9.67
1	11.77	22.34
2	17.41	24.59
3	25.3	32.22

which justifies the selection of SG6043 over NACA0012. When rotor rotated with three or higher rad/s, the torque for the blade with NACA0012 is comparable to SG6043, this is because rotor blade with SG6043 airfoil suffers much with the separated flow around the blade and it demands local pitch angle (θ) along the blade which is shown in Table 2.

5. Conclusions

The two-dimensional calculations of the SG6043 airfoil were performed using ANSYS-Fluent computational fluid dynamics (CFD) software and the results had been compared to the X-Foil software packages and wind tunnel test. It has been found that among various turbulent models available in the ANSYS-Fluent the k-ω shear stress transport (SST) model is in good agreement with X-Foil software packages and wind-tunnel test both for C_l and C_d.

Acknowledgments and funding

The author wishes to thank his colleagues and supervisor for his invaluable guidance. The financial support for this work provided by the Ministry of Human Resource Development, Government of India, is greatly appreciated.

References

[1] Khan MJ, Iqbal MT, Quaicoe JE. River current energy conversion systems: Progress, prospects and challenges. Renew Sustain Energy Rev 2008;12(8):2177–93.
[2] Swenson WJ. The Evaluation of an Axial Flow, Lift Type Turbine for Harnessing the Kinetic Energy in the Tidal Flow. Darwin, Australia: Australian Universities Power Engineering Conference AUPEC; 1999.
[3] Tiago GL. The State of the Art of Hydrokinetic Power in Brazil, Waterpower XIII. Buffalo: New York; 2003.

[4] Bahaj AS, Myers LE. Fundamentals applicable to the utilization of marine current turbines for energy production. Renew Energy 2003;28:2205–11.
[5] Khan MJ, Iqbal MT, Quaicoe JE. A Technology Review and Simulation-Based Performance Analysis of River Current Turbine Systems. Ottawa: IEEE CCECE/CCGEI; 2006.
[6] Khan MJ, Bhuyan G, Iqbal MT, Quaicoe JE. Hydrokinetic energy conversion systems and assessment of horizontal and vertical axis turbines for river and tidal applications: A technology status review. Appl Energy 2009;86(10):1823–35.
[7] Anyi M, Kirke BK. Hydrokinetic turbine blades: Design and local construction techniques for remote communities. Energy Sustain Dev 2011;15:223–30.
[8] Bahaj AS, Batten WMJ, McCann G. Experimental verifications of numerical predictions for the hydrodynamic performance of horizontal axis marine current turbines. Renew Energy 2007;(32):2479–90.
[9] Garman P. Water Current Turbines: A Fieldworker's Guide. UK: Intermediate Technology Publishing; 1986, ISBN: 0946688273.
[10] Giguere PaS. New airfoils for small horizontal axis wind turbines. ASME J Sol Eng 1998;120:108–14.
[11] Bahaj AS, Myers LE. Power output performance characteristics of a horizontal axis marine current turbine. Renew Energy 2006;31:197–208.
[12] Batten WMJ, Bahaj AS, Molland AF, Chaplin JR. The prediction of hydrodynamics of marine current turbines. Renew Energy 2008;33:1085–96.
[13] Massouh F, Dobrev I. Exploration of the vortex wake behind of wind turbine rotor. J Phys Conf Ser 2007;75:1–9.
[14] Manwell JF, McGowan JG. Wind Energy Explained: Theory, Design and Application. New York: John Wiley and Sons; 2002.
[15] ANSYS, Inc. Theory Guide. 2009.